A complex network-based approach to detecting and characterizing ictal states in patients with Childhood Absence Epilepsy

Paolo Lo Giudice*, Nadia Mammone†, Francesco Carlo Morabito‡, Davide Strati* and Domenico Ursino‡

*DIIES
UNIRC
I-89122 - Reggio Calabria - Italy
Email: {paolo.lo.giudice,davide.strati}@unirc.it

†IRCSS
Centro Neurolesi Bonino-Pulejo
I-98124 - Messina - Italy;
Email: nadia.mammone@irccsme.it

‡DICEAM
UNIRC
I-89122 - Reggio Calabria - Italy
Email: {morabito,ursino}@unirc.it

***Abstract*—This paper proposes a network analysis-based approach to detecting and characterizing ictal states in patients with Childhood Absence Epilepsy. Our approach defines and uses some suitable data structures, consisting of ad-hoc complex networks and subnetworks, and a new network analysis-based parameter, called connection coefficient. The examination of the values of this parameter on the adopted data structures allows our approach to reach its objectives. Obtained results are extremely encouraging and stimulate the extension of our approach in several directions.**

***Keywords*—Childhood Absence Epilepsy, Electroencephalogram, Complex Networks, Network Analysis, Connection Coefficient, Subnetworks**

I. Introduction

Nearly 1% of the world population is affected by epilepsy, a neurological disorder characterized by recurrent seizures. Epileptic seizures are still considered unpredictable, despite the huge efforts spent in recent years by scientific community to develop predictive algorithms. These are mainly based on electroencephalography, which consists in recording the scalp potentials produced by cortical electrical activity. Nearly 66% of patients can be successfully treated with anti-epileptic drugs, which have remarkable side effects, whereas nearly 8% of the drug-untractable patients are treated with surgery, which is high-invasive and high-risk. There is no way to treat the remaining 26% of patients.

In this paper, the attention is focused on Childhood Absence Epilepsy (CAE), an idiopathic generalized epileptic disorder [1], [2] characterized by recurrent "absence seizures" that cause disruption of awareness and are often associated with staring. Subjects experiencing absence seizures must undergo electroencephalography, which is a totally non-invasive and comfortable examination, consisting in recording the cortical electrical activity by means of scalp electrodes that are wired to an acquisition system, connected to a computer.

The electroencephalography acquisition can last from minutes to hours, depending on the number of recorded seizures and of the specific goal of the examination. In order to evaluate electroencephalograms (EEGs), a neurologist manually scrolls them, for detecting and inspecting every possible ictal state (seizure) or abnormality in the inter-ictal (seizure-free) activity. However, manual review is a time-consuming, inefficient and subjective procedure.

To expedite it and to facilitate the diagnosis, worldwide researchers are working to automatically mark the critical events occurring in an EEG, as well as to extract meaningful features from EEG signals, which can help a neurologist to make a diagnosis, to understand the pathology and, therefore, to optimize the treatment.

So far, many methodologies were proposed in the literature for the analysis of EEGs registering absence seizures. Permutation Entropy (PE), a symbolic complexity measure, was introduced in [3] and applied in [4] to analyze epileptic EEGs. Authors of [4] used PE to discriminate the different phases of epileptic activity in intracranial EEG time series, recorded from three intractable patients. In [5], PE was tested as a possible predictor of absence seizures in Genetic Absence Epilepsy Rats from Strasbourg (GAERS). PE outperformed Sample Entropy (SE) and detected the pre-ictal state in 169 out of 314 seizures from 28 rats, and the average anticipation time was $4.9s$. In [6], the authors exploited complexity analysis to detect vigilance changes in epileptic patients. In [7], Multiscale Permutation Entropy (MPE) was proposed to analyze human EEG signals at different absence seizure states. MPE, used in conjunction with Linear Discriminant Analysis (LDA), achieved a 90.6% sensitivity and exhibited a reduction of MPE levels from the inter-ictal state to the ictal one. In [8], the authors proposed Multi-Scale K-means (MSK-means) unsupervised learning to classify epileptic EEG signals and detect epileptic areas. In order to analyze the dynamics of EEG time series, while taking their mutual spatial dependence into account, a spatial-temporal analysis of epileptic EEGs was proposed in [9], [10], [11]. Due to the ability of PE in capturing the dynamics of EEGs registering absence seizures, a PE-based spatial-temporal analysis was proposed in [12], [13], [14]. Here, the authors showed that the frontal temporal lobes exhibited relatively high PE levels, whereas the parieto-occipital areas appeared associated with relatively low PE values. However, being PE univariate, it is only able to quantify the randomness of single EEG channels independently; instead, it is not able to quantify the interaction between channels. To investigate this

last issue, the necessity arises of bivariate descriptors, which can provide an estimation of the interaction between channels.

Among this last kind of descriptors, *coherence* is one of the most promising [15]. As a matter of fact, in [16], Partial Directed Coherence (PDC) was employed to quantify the strength and the direction of the interactions between the electrodes during the inter-ictal (i.e., seizure free) EEG segments in CAE patients. PDC revealed an abnormal cortical network activity during the inter-ictal state, in particular in the alpha band. In [17], the authors proposed a method consisting of a three level wavelet decomposition, a coherence estimation and a phase synchrony feature extraction to classify ictal vs inter-ictal EEG segments.

Since absence ictal states appear associated with an increased EEG synchronization, coherence revealed a powerful descriptor of absence seizure EEG signals [16], [15]. In [15], the authors constructed EEG networks, based on the estimation of coherence and Synchronization Likelihood (SL), to investigate the network changes associated with seizure onset. Ictal EEG segments were characterized by an increased synchronization and a more ordered network topology. In [18], the authors applied PDC-based weighted directed graph analysis to EEGs of patients with absence seizures to perform a classification of nodes (electrodes) according to their source/sink nature.

This paper aims at providing a contribution in this setting. In fact, it studies the temporal variation of the synchronization between EEG signals to automatically discriminate ictal vs inter-ictal states, while keeping the global view of how these temporal variations involve the different areas of the cortex. For this purpose, an EEG-based complex network model was developed, where nodes represent electrodes (i.e., cortical areas) and the weight of edges represents the complementary of the coherence value between the EEG signals, recorded at the electrodes associated with the corresponding nodes. A complex network-analysis was carried out to find possible changes in the network features driven by the onset of epileptiform activity. By studying the behavior of the network and its subnetworks over time, a global evaluation of the behavior of the cortex is possible, and the presence of seizures can be automatically detected.

The proposed approach differs significantly from previous studies related to EEGs with absence seizure. To our best knowledge, this is the first time that social network analysis is applied to the EEG of patients with absence seizures. Furthermore, in previous studies, based on the use of complex networks for the detection of absence ictal states, for every patient, only one seizure was manually selected [15], whereas, in the present work, all the recorded seizures are considered, and an overall accuracy is achieved for every patient. In our approach, the whole EEG recording is segmented into overlapping windows and, then, it is processed window by window, so that an overall and smooth analysis of it is achieved. Moreover, no artifact rejection preprocessing was carried out in order to introduce no discontinuity in the dataset and to track the dynamics of the EEG time series continuously. Furthermore, a novel complex network parameter, called connection coefficient, is introduced. It proved particularly adequate to quantify the connection level of a network. The present paper is mainly methodological as it introduces a novel approach for the analysis of EEGs with absence seizures. However, since preliminary results, achieved over a dataset of 9 CAE patients, are very encouraging, the proposed method will be tested on a larger dataset in the near future.

This paper is organized as follows: in Section II, we describe available data and define coherence. In Section III, we introduce some support data structures employed by our approach. Section IV represents the core of this paper, because it illustrates our approach. Finally, in Section V, we draw our conclusions and give a look at some future developments of this research.

II. Available data

A. EEG recording and preprocessing

A dataset including 9 EEG recordings from patients diagnosed with CAE was studied. The children mean age was 7.44 years, with a standard deviation of 1.67 years. The average duration of EEG recordings was 25.68 mins.

The dataset was provided by $UNEEG^{TM}$ medical A/S (Lynge, Denmark) within a research cooperation agreement. The EEG montage was set according to the international 10/20 system. EEGs were recorded by means of Stellate Harmonie (Stellate Systems, Inc., Montreal, Quebec, Canada) and Cadwell Easy II (Cadwell Laboratories, Inc., Kennewick, WA) systems. EEG traces were reviewed by a board-certified epileptologist, who marked all the paroxysms.

The method flowchart can be described as follows: 1) the *n*-channels EEG is recorded, band-pass filtered between 0.5 and 32 Hz (because absence seizure activity mainly lies in this range [19]), digitized with a sampling rate of 200 Hz and stored on a computer; 2) the EEG is segmented into *M* overlapping windows (with $2s$ width and $1s$ overlap) and analyzed window by window; 3) given the k^{th} window *EEG(k)* (where $k = 1, \ldots, M$), the complementary $1 - C_{v_i,v_j}$ of the coherence between every pair of electrodes (v_i, v_j) is estimated, and used as the weight of the edge between the nodes corresponding to v_i and v_j.

The width of the overlapping windows was set at $2s$ because the paroxysms longer than $2s$ are those considered to be clinically relevant. The $1s$ overlap ensures that the EEG is processed smoothly and that there is no abrupt variation in estimated descriptors. EEG processing was implemented and carried out in MATLAB R2016b (The MathWorks, Inc., Natick, MA, USA).

B. Coherence estimation

The magnitude squared coherence between two signals v_i and v_j depends on the frequency f and is defined as:

$$C_{v_i,v_j}(f) = \frac{|P_{v_i,v_j}(f)|^2}{P_{v_i,v_i}(f)P_{v_j,v_j}(f)}$$

where $P_{v_i,v_i}(f)$ and $P_{v_j,v_j}(f)$ are the Power Spectral Densities (PSD) of v_i and v_j, respectively, whereas $P_{v_i,v_j}(f)$ represents the cross power spectral density between v_i and v_j. Coherence C_{v_i,v_j} is a measure of synchronization between v_i and v_j and is bounded between 0 and 1. In this work, it was estimated using the method of Welch's averaged, modified periodogram [20].

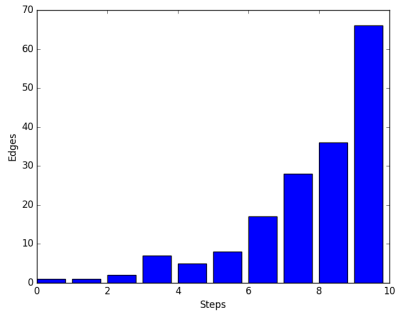

Fig. 1. Average edge weight distribution in inter-ictal states

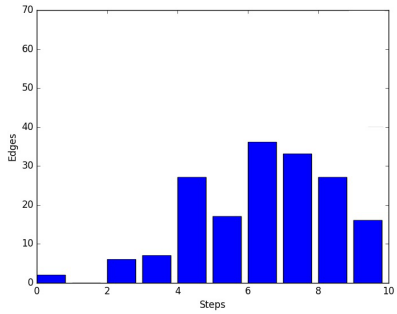

Fig. 2. Average edge weight distribution in ictal states

The k^{th} EEG window under analysis, and the estimated values of coherence $C^k_{v_i,v_j}(f)$ for every frequency f, were averaged over the frequencies of the range under consideration (f_L=0.5 Hz - f_U=32 Hz):

$$\overline{C}^k_{v_i,v_j} = \frac{1}{f_U - f_L} \int_{f_L}^{f_U} C^k_{v_i,v_j}(f) df$$

Therefore, for every analyzed window *EEG(k)*, and for every pair of electrodes (v_i, v_j), an average value of coherence $\overline{C}^k_{v_i,v_j}$ is computed.

III. Support data structures

Let eeg be a generic EEG. Starting from it, a network (that we call *brain network*) $\mathcal{N} = \langle V, E \rangle$ can be defined.

Here, V is the set of nodes of $\mathcal{N}$. Each node $v_i \in V$ corresponds to an electrode. In our EEGs, electrodes were applied by following the 10-20 system and $|V| = 19$.

E is the set of edges of $\mathcal{N}$. Each edge e_{ij} connects nodes v_i and v_j. It can be represented as $e_{ij} = (v_i, v_j, w_{ij})$. Here, w_{ij} is a measure of "distance" between v_i and v_j. It is an indicator of the disconnection level of v_i and v_j. Indeed, each measure representing this feature could be adopted in our model. In the experiments presented in this paper, we employed the complementary of the coherence value between v_i and v_j (i.e., we set $w_{ij} = 1 - C_{v_i,v_j}$).

A preliminary investigation performed in our research consisted of determining the edge weight distribution (averaged on all available patients) in ictal, pre-ictal, post-ictal and inter-ictal states, even if, in this paper, our focus is on ictal and inter-ictal states. In carrying out this task, we separated the range of edge weights (which, we recall, is $[0, 1]$) in ten intervals of the same length. The obtained distribution for inter-ictal and ictal states is reported in Figures 1 and 2. From a deeper evaluation of these distributions, we can observe that there are some intervals more relevant than others for distinguishing the two states. As a consequence, to better detect and characterize ictal states, it is reasonable to consider some ad-hoc subnetworks, each taking only the edges belonging to specific intervals into account.

In particular, we defined the following subnetworks: $\mathcal{N}^b = \langle V, E^b \rangle$, $\mathcal{N}^m = \langle V, E^m \rangle$, $\mathcal{N}^r = \langle V, E^r \rangle$, $\mathcal{N}^g = \langle V, E^g \rangle$, $\mathcal{N}^y = \langle V, E^y \rangle$, $\mathcal{N}^{br} = \langle V, E^{br} \rangle$. We used a color name to provide a more mnemonic way of distinguishing sub-networks. Thus, the superscripts b, m, r, g, y, br stand for *blue, magenta, red, green, yellow* and *brown*, respectively.

Given that the set of nodes is the same for all subnetworks, we focus on defining only the set of edges of each of them:

$$\begin{aligned}
E^b &= \{e_{ij} \mid e_{ij} \in E, 0.9 < w_{ij} \leq 1\},\\
E^m &= \{e_{ij} \mid e_{ij} \in E, 0.8 < w_{ij} \leq 0.9\},\\
E^r &= \{e_{ij} \mid e_{ij} \in E, 0.7 < w_{ij} \leq 0.8\},\\
E^g &= \{e_{ij} \mid e_{ij} \in E, 0.6 < w_{ij} \leq 0.7\},\\
E^y &= \{e_{ij} \mid e_{ij} \in E, 0.5 < w_{ij} \leq 0.6\},\\
E^{br} &= \{e_{ij} \mid e_{ij} \in E, 0.3 < w_{ij} \leq 0.4\}.
\end{aligned}$$

Finally, we constructed two further subnetworks. The former was obtained by merging *blue*, *magenta*, *red*, *green* and *yellow* subnetworks (we called "*rainbow*" this network). The latter was constructed by considering all the edges of the original network not belonging to the *rainbow* one (we called "*black*" this network). Formally speaking, the two networks are defined as: $\mathcal{N}^{rbw} = \langle V, E^{rbw} \rangle, \mathcal{N}^{blk} = \langle V, E^{blk} \rangle$, where:

$$\begin{aligned}
E^{rbw} &= \{e_{ij} \mid e_{ij} \in E, 0.5 < w_{ij} \leq 1\},\\
E^{blk} &= \{e_{ij} \mid e_{ij} \in E, 0 \leq w_{ij} \leq 0.5\}.
\end{aligned}$$

Since each EEG is in the form of a time series, it could be useful to introduce the concept of *mean network*. Thus, given q networks $\mathcal{N}_1 = \langle V, E_1 \rangle$, $\mathcal{N}_2 = \langle V, E_2 \rangle$, $\cdots$, $\mathcal{N}_q = \langle V, E_q \rangle$, we define the *mean network* $\overline{\mathcal{N}}$, corresponding to them, as: $\overline{\mathcal{N}} = \langle V, \overline{E} \rangle$, where:

$$\overline{E} = \{(v_i, v_j, \overline{w}_{ij}) \mid e_{ij_k} = (v_i, v_j, w_{ij_k}) \in E_k, 1 \leq k \leq q, \overline{w}_{ij} = \frac{\sum_{k=1}^{q} w_{ij_k}}{q}\}.$$

Observe that $0 \leq \overline{w}_{ij} \leq 1$.

IV. Detection and characterization of ictal states

A. Connection coefficient

As pointed out before, one of the main features to investigate for the detection of ictal states is the connection level of the brain areas. In network analysis, one of the most powerful tools for investigating the connection level of a network is the concept of clique [21]. Starting from cliques, it is possible to define a quantitative coefficient, which we call *connection coefficient*, capable of measuring the connectivity level of a network associated with an EEG. This coefficient takes the following considerations into account: *(i)* both the dimension

and the number of cliques are important as connectivity indicators; *(ii)* the concept of clique is intrinsically exponential; in other words, a clique of dimension $n+1$ is exponentially more complex than a clique of dimension n. We are now able to define the connection coefficient $cc_{\mathcal{N}}$ of a network $\mathcal{N}$. In particular, let $\mathcal{C}$ be the set of the cliques of $\mathcal{N}$; let $\mathcal{C}_k$ be the set of cliques of dimension k of $\mathcal{N}$; finally, let $|\mathcal{C}_k|$ be the cardinality (i.e., the number of cliques) of $\mathcal{C}_k$. Then, $cc_{\mathcal{N}}$ is defined as:

$$cc_{\mathcal{N}} = \sum_{k=1}^{|V|} |\mathcal{C}_k| \cdot 2^k$$

B. Detecting ictal states

Detecting ictal states is a very delicate and time consuming task for a neurologist, who have to analyze a whole EEG. Our effort, in this case, was to compute, on a time-slot base, the value of the connection coefficient for an EEG. And so, for each patient and each time-slot, we computed the value of the connection coefficient of the brain network associated with the EEG at that time-slot.

Indeed, in order to better evidence this phenomenon, we considered the brain subnetworks $\mathcal{N}^{rbw}$ and $\mathcal{N}^{blk}$, defined in Section IV. We recall that $\mathcal{N}^{rbw}$ considers the five intervals of edge distribution characterized by the heaviest weights, whereas $\mathcal{N}^{blk}$ encompasses the other ones. As a consequence, since edge weights represent distances, on the basis of the results of [15], we can expect that, in presence of an ictal state, the connection coefficient associated with $\mathcal{N}^{rbw}$ presents a minimum, whereas the one corresponding to $\mathcal{N}^{blk}$ shows a maximum. This is explained by the fact that, during the ictal states, the weights of the edges tend to decrease and, therefore, several edges disappear from $\mathcal{N}^{rbw}$ and appear in $\mathcal{N}^{blk}$. For the sake of brevity, we will only look at the results obtained for Patient 18 as an example, but we obtained very similar results for all of the other patients.

In Table I, we report data about figures specified by an expert neurologist when she examined the whole EEG of Patient 18. The physician identified 8 seizures, which took place into the time-slots specified in this table.

TABLE I. TABLE PRODUCED BY A NEUROLOGIST ABOUT START AND END TIME-SLOTS FOR EACH SEIZURE OF PATIENT 18

Seizure id	*Start time-slot*	*End time-slot*
1	4	26
2	120	122
3	165	205
4	306	332
5	449	451
6	470	496
7	642	659
8	891	913

We use this table as a starting point and a benchmark of accuracy for the detection of ictal states performed by our approach.

In Figure 3, we plotted the values of the connection coefficient (y axis) for each time-slots (x axis) for Patient 18 and for $\mathcal{N}^{rbw}$, whereas, in Figure 4, we represented the values of the same coefficient for the same patient, but for $\mathcal{N}^{blk}$.

Clearly, in Figure 3 it is straightforward to observe that there are some time-slots in which connection coefficient is

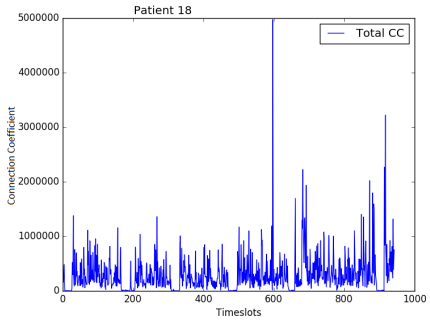

Fig. 3. Connection coefficient for the network $\mathcal{N}^{rbw}$ of Patient 18

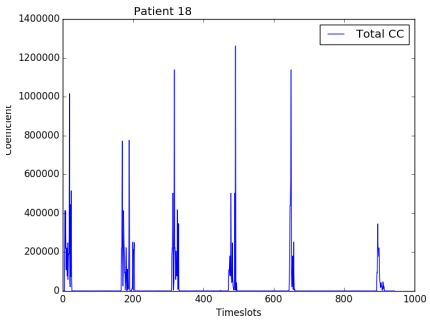

Fig. 4. Connection coefficient for the network $\mathcal{N}^{blk}$ of Patient 18

several orders of magnitude less than others. The important result is that those time-slots are exactly the ones that the neurologist spotted as ictal states. For instance, in Figures 5 and 6, we show more closely the part of the plot of Figure 3 corresponding to the first and the eighth seizures, in such a way as to allow the reader to more appreciate the differences, in terms of magnitude, of the value of connection coefficient in the involved states.

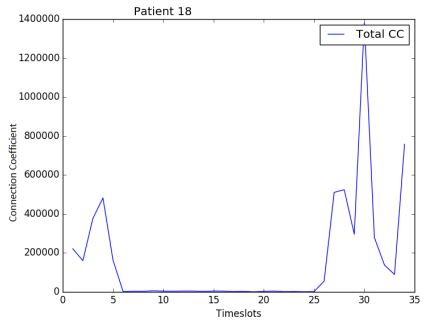

Fig. 5. Zoomed plot of the value of connection coefficient of Figure 3 - first seizure

Thus, without having to manually analyze the whole EEG for a patient, thanks to this coefficient, we can easily distinguish ictal states from the others.

In order to provide a quantitative evaluation of the performance of our approach, we computed its sensitivity, specificity and precision for each patient and, then, for the set of seizures of all patients, taken as a whole. Obtained results are reported in Table II. Taking into account that, in this application

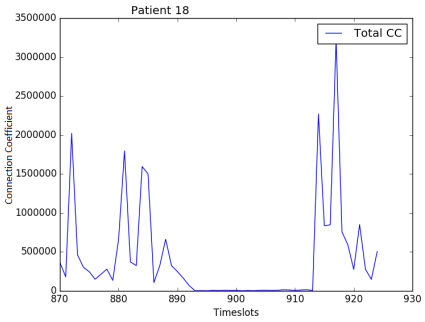

Fig. 6. Zoomed plot of the value of connection coefficient of Figure 3 - eighth seizure

context, sensitivity is more important than specificity, we have considered the union of the seizures detected by using $\mathcal{N}^{rbw}$ and $\mathcal{N}^{blk}$.

TABLE II. SENSITIVITY, SPECIFICITY AND PRECISION OF OUR APPROACH

Patient	*Sensitivity*	*Specificity*	*Precision*
16	0.9032	0.8400	0.7272
18	1.0000	0.9291	0.9961
23	0.9629	0.9882	0.9167
29	1.0000	0.9483	0.9473
31	1.0000	0.9287	0.9438
32	1.0000	0.9356	0.8644
39	1.0000	0.8642	0.7400
47	1.0000	0.9610	0.9917
57	1.0000	0.9012	0.4375
Overall	0.9704	0.9169	0.6482

From the analysis of this table, we can see that our approach provides excellent results, especially if we look at sensitivity. However, also specificity and precision are very good. Clearly, we are conscious that the number of examined patients is small. However, as previously pointed out, due to the encouraging results obtained, and due the *methodological nature* of our paper, we believe the present research can contribute to motivate clinical centers to engage an experimentation of our approach with a much higher number of patients.

C. Characterizing ictal states

In order to understand and characterize what happens during *ictal states*, we analyzed the subnetworks defined in Section III. For this purpose, we computed a mean network for each inter-ictal time-slot, up to 40 time slots before the seizures, and we mediated those networks among all patients. We did the same task for ictal time-slots, up to 8 time-slots after the start of a seizure, until the *center-ictal time-slot*.

The subnetworks we used were the blue one $\mathcal{N}^b$, the magenta one $\mathcal{N}^m$, the red one $\mathcal{N}^r$, the green one $\mathcal{N}^g$, the yellow one $\mathcal{N}^y$ and the brown one $\mathcal{N}^{br}$. We computed the values of connection coefficient for each colored subnetwork of the mean networks previously derived. Obtained results are plotted in Figure 7. Here, we show the average connection coefficient of some colored networks for 40 time-slots of inter-ictal state and 8 time-slots of ictal state.

As we can see from this figure, during the inter-ictal state, the values of connection coefficient do not deeply change until the first time-slot before *ictal*. At this time, we can see that the values of connection coefficient increase for yellow and green subnetworks and become higher than the corresponding ones of magenta and blue subnetworks. An increase of the values of connection coefficient for yellow and green subnetworks, coupled with a strong decrease of the values of this coefficient for blue and magenta subnetworks, implies that, during ictal states, both the number and the dimension of the cliques in yellow and green subnetworks increase, whereas the corresponding ones in blue and magenta subnetworks decrease. In turn, this implies that a certain number of edges migrate from magenta and blue subnetworks to green and yellow ones. Now, recall that yellow and green edges have a weight between 0.5 and 0.7, whereas magenta and blue edges have a weight between 0.8 and 1. As a consequence, the edge migration described above implies that a hyper-synchronization of brain areas happens during ictal states.

This characterization result for ictal state is particularly interesting because we were able to confirm, through a network analysis-based approach, what several authors had found in the past, through completely different approaches (see, for instance, [15]), namely that ictal states are characterized by hyper-synchronization, which can be automatically detected. With reference to this feature, it is worth emphasizing that we evaluated the sensitivity and the specificity of the proposed approach over the whole EEG recording, and not over selected epochs, which makes our approach suitable for possible real-time applications. Interestingly, in our tests, no artifactual epoch was discarded, in order to track the behavior of the EEG continuously and to evaluate the sensitivity, specificity and precision of our approach in real conditions, when noise and artifacts may be present. Furthermore, the usage of complex networks allows the investigation of the interactions between the different areas of the brain in absence and in presence of a seizure, which we aim at deepening in the future. Finally, we point out that, at the moment, the system can be used off-line to mark the seizures automatically and allow the neurologist to skip the manual EEG review, which is extremely time consuming. However, we plan to optimize it in the future in such a way as to allow for a continuous, real time, long-term monitoring.

V. CONCLUSION

In this paper, we have presented a network analysis-based approach to detecting and characterizing ictal states in patients with CAE. Our approach associates one or more complex networks and subnetworks with each EEG at disposal. To reach its objective, it introduces a new parameter, called connection coefficient, and evaluates this parameter on each available network and some ad-hoc subnetworks, defined in such a way as to maximally evidence the differences between inter-ictal and ictal states. Obtained results are extremely encouraging, as shown in Sections IV-B and IV-C.

In the future, we plan to extend our approach in several directions. First, we would like to make it capable of detecting and characterizing pre-ictal states, which is a much more complex but, at the same time, extremely useful task. Then, we plan to extend our approach to investigate the mechanisms of area recruitment that occur in the inter-ictal and pre-ictal states. Furthermore, we plan to construct a dashboard of parameters

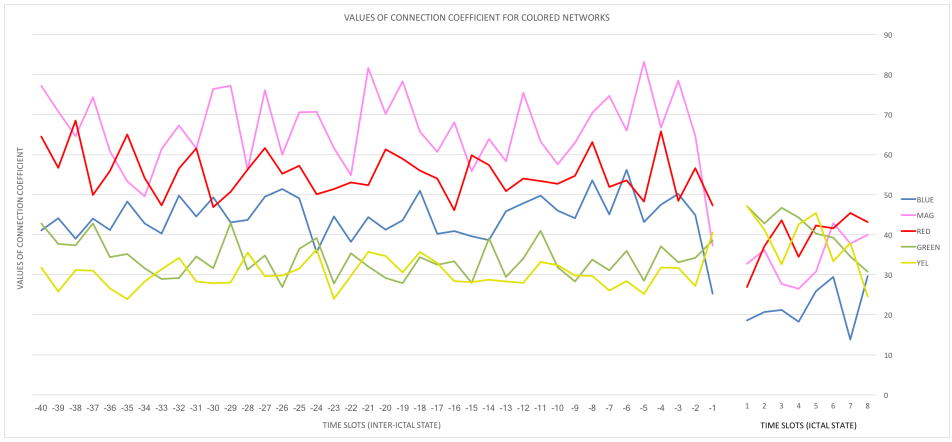

Fig. 7. Connection Coefficient for mean networks during pre-ictal and ictal states

(instead of the only connection coefficient) to adopt for the detection and the characterization of ictal and pre-ictal states. Last, but not the least, we plan to make our approach able to handle other forms of epilepsy.

ACKNOWLEDGEMENTS

Nadia Mammone's work was funded by the Italian Ministry of Health, Project Code GR-2011-02351397. This work was partially supported by Aubay Italia S.p.A.

The EEG data and the medical feedback were kindly provided by T. W. Kjaer (Center of Neurophysiology, Department of Neurology, at Zealand University Hospital, Roskilde, Denmark) and J. Duun-Henriksen ($UNEEG^{TM}$ medical A/S, Nymollevej 6, DK-3540, Lynge, Denmark).

REFERENCES

[1] J. Duun-Henriksen, R. Madsen, L. Remvig, C. Thomsen, H. Sorensen, and T. Kjaer, "Automatic detection of childhood absence epilepsy seizures: toward a monitoring device," *Pediatric Neurology*, vol. 46, no. 5, pp. 287–292, 2012.

[2] J. Duun-Henriksen, T. Kjaer, R. Madsen, L. Remvig, C. Thomsen, and H. Sorensen, "Channel selection for automatic seizure detection," *Clinical Neurophysiology*, vol. 123, no. 1, pp. 84–92, 2012.

[3] C. Bandt and B. Pompe, "Permutation entropy: A natural complexity measure for time series," *Physical review letters*, vol. 88 (17), p. 174102, 2002.

[4] Y. Cao, W. Tung, J. Gao, V. Protopopescu, and L. Hively, "Detecting dynamical changes in time series using the permutation entropy," *Physical Review E*, vol. 70, p. 046217, 2004.

[5] X. Li, G. Ouyang, and A. Douglas, "Predictability analysis of absence seizures with permutation entropy," *Epilepsy Research*, vol. 77, pp. 70–74, 2007.

[6] A. Bruzzo, B. Gesierich, M. Santi, C. Tassinari, N. Birbaumer, and G. Rubboli, "Permutation entropy to detect vigilance changes and preictal states from scalp EEG in epileptic patients. a preliminary study," *Neurological Science*, vol. 29(1), pp. 3–9, 2008.

[7] G. Ouyang, J. Li, X. Liu, and X. Li, "Dynamic characteristics of absence EEG recordings with multiscale permutation entropy analysis," *Epilepsy Research*, vol. 104, no. 3, pp. 246–252, 2013.

[8] G. Zhu, Y. Li, P. Wen, and S. Wang, "Classifying epileptic EEG signals with delay permutation entropy and multi-scale k-means," *Advances in Experimental Medicine and Biology*, vol. 823, pp. 143–157, 2015.

[9] N. Mammone, J. Principe, F. Morabito, D. Shiau, and J. Sackellares, "Visualization and modelling of STLmax topographic brain activity maps," *Journal of neuroscience methods*, vol. 189, no. 2, pp. 281–294, 2010, Elsevier.

[10] N. Mammone, F. L. Foresta, G. Inuso, F. Morabito, U. Aguglia, and V. Cianci, "Algorithms and topographic mapping for epileptic seizures recognition and prediction," *Frontiers in Artificial Intelligence and Applications*, no. 204, pp. 261–270, 2009, IOS Press.

[11] N. Mammone, F. L. Foresta, and F. Morabito, "Discovering network phenomena in the epileptic electroencephalography through permutation entropy mapping," *Frontiers in Artificial Intelligence and Applications*, vol. Neural Nets WIRN10, pp. 260–269, 2011, IOS Press.

[12] N. Mammone and F. Morabito, "Analysis of absence seizure eeg via permutation entropy spatio-temporal clustering," in *Proceedings of the International Joint Conference on Neural Networks (IJCNN 2011)*, San Jose, CA, USA, 2011, pp. 1417–1422, IEEE.

[13] N. Mammone, J. Henriksen, T. Kjaer, and F. Morabito, "Differentiating interictal and ictal states in childhood absence epilepsy through Permutation Renyi Entropy," *Entropy*, vol. 17, no. 7, pp. 4627–4643, 2015.

[14] N. Mammone, J. Duun-Henriksen, T. Kjaer, M. Campolo, F. L. Foresta, and F. Morabito, "Quantifying the complexity of epileptic eeg," in *Smart Innovation, Systems and Technologies: Advances in Neural Networks*, 2016, pp. 223–232, Springer.

[15] S. Ponten, L. Douw, F. Bartolomei, J. Reijneveld, and C. Stam, "Indications for network regularization during absence seizures: weighted and unweighted graph theoretical analyses," *Experimental Neurology*, vol. 217, no. 1, pp. 197–204, 2009, Elsevier.

[16] F. Rotondi, S. Franceschetti, G. Avanzini, and F. Panzica, "Altered EEG resting-state effective connectivity in drug-naïve childhood absence epilepsy," *Clinical Neurophysiology*, vol. 127, no. 2, pp. 1130–1137, 2016.

[17] D. Ravish, S. Devi, and S. G. S.G. Krishnamoorthy, "Wavelet analysis of EEG for seizure detection: Coherence and phase synchrony estimation." *Biomedical Research*, 2015, Biomedical Research.

[18] A. Rodrigues, B. Machado, L. Caboclo, A. Fujita, L. Baccaia, and K. Sameshima, "Source and sink nodes in absence seizures," in *Proceedings of the Annual International Conference of the IEEE Engineering in Medicine and Biology Society (EMBS'16)*, Orlando, FL, USA, 2016, pp. 2814–2817, IEEE Society.

[19] J. Gotman, J. Ives, and P. Gloor, "Frequency content of EEG and EMG at seizure onset: possibility of removal of textscEMG artefact by digital filtering," *Electroencephalography and clinical neurophysiology*, vol. 52, no. 6, pp. 626–639, 1981, Elsevier.

[20] P. Welch, "The Use of Fast Fourier Transform for the Estimation of Power Spectra: A Method Based on Time Averaging Over Short, Modified Periodograms," *IEEE Transactions on Audio and Electroacoustics*, vol. 15, no. 2, pp. 70–73, 1967.

[21] M.Tsvetovat and A. Kouznetsov, *Social Network Analysis for Startups: Finding connections on the social web*, 2011, o'Reilly Media, Inc.